https://doi.org/10.31925/farmacia.2026.1.13 **ORIGINAL ARTICLE**

EXPLORING THE EFFECTS OF DELPHINIDIN TREATMENT ON BROWNING PROCESSES IN 3T3-L1 PREADIPOCYTE CELLS: A FOODOMICS APPROACH

ELİF DİDEM ÖRS DEMET [1, 2], KÜBRA UÇAR BAŞ [2], ASLIHAN ALPASLAN [2], DİLEM TUGAL ASLAN [2], TUBA RECBER [3], TUGBA GULSUN [4], MUSTAFA ÇELEBİER [3], ZEYNEP GÖKTAŞ [2]*

[1]*Department of Nutrition and Dietetics, Nezahat Keleşoğlu Faculty of Health Sciences, Necmettin Erbakan University, Konya, Türkiye*
[2]*Department of Nutritional Sciences, Faculty of Health Sciences, Hacettepe University, Ankara 06100, Türkiye*
[3]*Department of Analytical Chemistry, Faculty of Pharmacy, Hacettepe University, Ankara 06100, Türkiye*
[4]*Department of Pharmaceutical Technology, Faculty of Pharmacy, Hacettepe University, Ankara 06100, Türkiye*

**corresponding author: zeynep.goktas@hacettepe.edu.tr*

Manuscript received: November 2025

Abstract

Foodomics uses advanced omics technologies to evaluate the molecular effects of food components in organisms. Delphinidin, a valuable polyphenol anthocyanidin, has demonstrated protective effects against obesity-related conditions, making it a promising candidate for dietary supplements. The purpose of this study was to investigate the effects of delphinidin treatment (5, 10, and 20 μM) on 3T3-L1 preadipocytes in relation to thermogenesis and browning processes. The cells were treated in two distinct stages of adipocyte formation: during differentiation and the subsequent maturation process. To achieve this, we evaluated the expression of the main protein markers (*UCP1*, *PGC1-α*, and *PPARγ*) and genes correlated with browning (*UCP1*, *PPARγ*, *C/EBPβ*, *PGC1-α*, *CIDEA*, *FABP4*, and *PRDM16*) as well as those related to lipid metabolism. A GC-MS-based metabolomics method was used to understand delphinidin's effects at the lipid level. The results suggest that delphinidin may contribute to the browning of adipose tissue through regulators such as *UCP1* and *PRDM16*, while not affecting *PPARγ*, *C/EBPβ*, and *FABP4*. The foodomics approach, which integrates multi-omics data, indicates that delphinidin interacts across different metabolic pathways, influencing metabolites such as glyceraldehyde, alanine, and porphine. These findings offer a strong basis for the development of obesity therapeutics through dietary supplements, though further studies are required to confirm delphinidin's browning effects.

Rezumat

Foodomica utilizează tehnologii omice avansate pentru a evalua efectele moleculare ale componentelor alimentare în organisme. Delfinidina, un polifenol din clasa antocianidinelor, a demonstrat efecte protectoare împotriva afecțiunilor asociate obezității, ceea ce o face un candidat promițător pentru suplimente alimentare. Scopul acestui studiu este de a investiga efectele tratamentului cu delfinidină (5, 10 și 20 μM) asupra preadipocitelor 3T3-L1, în relație cu termogeneza și procesele de brunificare. Celulele au fost tratate în două etape distincte ale formării adipocitelor: în timpul diferențierii și în procesul ulterior de maturare. Pentru a realiza acest lucru, au fost evaluate expresiile principalilor markeri proteici (*UCP1*, *PGC1-α* și *PPARγ*) și ale genelor corelate cu brunificarea (*UCP1*, *PPARγ*, *C/EBPβ*, *PGC1-α*, *CIDEA*, *FABP4* și *PRDM16*), precum și cele implicate în metabolismul lipidic. O metodă metabolomică bazată pe GC/MS a fost utilizată pentru a înțelege efectele delfinidinei la nivel lipidic. Rezultatele sugerează că delfinidina poate contribui la brunificarea țesutului adipos prin intermediul regulatorilor precum *UCP1* și *PRDM16*, fără a influența *PPARγ*, *C/EBPβ* și *FABP4*. Abordarea foodomică, care integrează date multi-omice, indică faptul că delfinidina interacționează în diferite căi metabolice, influențând metaboliți precum gliceraldehida, alanina și porfina. Aceste constatări oferă o bază solidă pentru dezvoltarea de terapii anti-obezitate prin suplimente alimentare, deși sunt necesare studii suplimentare pentru a confirma efectele de brunificare ale delfinidinei.

Keywords: delphinidin, obesity, foodomics, adipocyte browning, *UCP1*

Introduction

"Foodomics" integrates advanced omics technologies, like transcriptomics, metabolomics, and proteomics, with biostatistics, bioinformatics, and chemometrics to assess complex biological systems and their interaction with bioactive food compounds (1). Recent omics technologies are used to explore how phytochemicals, secondary metabolites from plants, can positively affect human health by altering protein levels, functions, and gene expressions, and reducing disease risk (2). Delphinidin (2-(3, 4, 5-trihydroxyphenyl) chromenylium-3, 5, 7-triol) is an anthocyanidin-type polyphenol (3). It belongs to the anthocyanidin subgroup of polyphenols, a subfamily of flavonoids, that includes different varieties as follows: cyanidin, malvidin, pelargonidin, delphinidin, peonidin, and petunidin (4). Recent studies have reported that delphinidin may be protective against obesity-related conditions such as oxidative stress,

inflammation, insulin resistance, and steatosis by altering redox signalling in mice fed a high-fat diet (5, 6). In an animal study, Maqui berry supplementation with high amounts of delphinidin as an anthocyanin was shown to improve insulin response and reduce weight gain (7). Delphinidin shows promise in reducing intracellular lipid accumulation, promoting lipolysis, and regulating adipogenic genes, which could help prevent metabolic diseases like obesity (8). Similar studies suggest that black soybean anthocyanins, primarily containing delphinidin, also benefit obesity by inhibiting adipocyte differentiation and stimulating lipolysis while reducing adipogenesis (9-11). Delphinidin inhibits *PPARγ* expression, leading to lower 3T3-L1 cell viability and differentiation (9). Moreover, supplementation of C57BL/6 mice with blueberry and mulberry juice containing delphinidin, the major anthocyanin, for 12 weeks inhibited weight gain, reduced serum cholesterol levels, insulin resistance, leptin levels, and lipid accumulation, and thus may prevent obesity (12). However, only a limited number of *in vitro*, *in vivo*, and human studies have been conducted thus far, and it is premature to generalize that the consumption of delphinidin consistently leads to favourable effects. Further studies are necessary because its molecular and metabolic effects and safety profile are not fully understood. This study aimed to evaluate the effects of delphinidin on thermogenesis and browning processes in 3T3-L1 preadipocytes with a foodomics approach.

Materials and Methods

Materials

Delphinidin (≥ 97% purity) was purchased from Cayman Chemical Co. Cholesterol, 3-isobutyl-L-methylxanthine (IBMX), insulin, dimethyl Sulfoxide (DMSO), Dulbecco's modified Eagle's medium (DMEM), bovine calf serum (BCS), trypsin-EDTA, and fetal bovine serum (FBS) were purchased from Merck (Sigma-Aldrich). Dexamethasone (DEX) was purchased from Cayman Chemical Co. 3T3-L1 preadipocyte cells were purchased from ATCC.

Cell culture

3T3-L1 preadipocyte cells were grown in Dulbecco's modified Eagle's medium (DMEM) containing 10% FBS, penicillin (100 U/mL), and streptomycin (100 µg/mL) at 37°C in a humidified atmosphere of 5% CO_2. Adipocyte differentiation was initiated two days post-confluence (designated as Day 0) by supplementing the culture medium with 0.5 mM IBMX, 1 µM dexamethasone (DEX), and 10 µg/mL insulin. After 48 h (Day 2), the medium was replaced with DMEM containing 10 µg/mL insulin, which was refreshed every two days until full maturation (Day 8).

To evaluate the effects of delphinidin on adipocyte biology, two distinct treatment paradigms were applied: (1) Differentiation-phase treatment: Cells were treated with delphinidin (5, 10, or 20 µM) continuously from Day 0 to Day 8, with delphinidin replenished at each medium change; (2) Maturation-phase treatment: Fully differentiated adipocytes (Day 8) were treated with delphinidin (5, 10, or 20 µM) for an additional 48 h (Day 8 - 10).

Control cells received vehicle (PBS) only and were processed in parallel for both experimental phases.

To allow clear temporal interpretation of molecular and metabolic outcomes, gene expression, protein abundance, triglyceride content, and metabolomic profiling were assessed separately at defined time points. For the differentiation-phase experiments, cells were harvested at Day 8. For the maturation-phase experiments, cells were harvested after 48 h of treatment at Day 10.

All downstream analyses were performed using samples collected at these respective endpoints, and datasets derived from differentiation and maturation phases were analyzed independently.

Measuring gene expression levels

Total RNA was isolated using an RNA extraction kit. RNA concentration and purity were assessed spectrophotometrically by measuring absorbance at 260 and 280 nm. Equal amounts of RNA (1 µg *per* sample) were reverse-transcribed into cDNA using the OneScript® Plus cDNA Synthesis Kit according to the manufacturer's instructions. Reverse transcription was performed in a total reaction volume of 20 µL using a blend of oligo(dT) and random primers. The reaction conditions consisted of incubation at 42°C for 30 min, followed by enzyme inactivation at 85°C for 5 min, using Piko® Thermal Cyclers.

Quantification of gene expression was performed using LightCycler 480. Amplification was performed for each target gene using 4 µL cDNA, 1 µL primer (forward and reverse), 10 µL BlasTaq™ 2X qPCR MasterMix, and 5 µL deionized water. The expression levels of the genes (*PPARγ*, *C/EBPβ*, *PGC1-α*, *CIDEA*, *FABP4*, *UCP1*, *PRDM16*) were normalized to β-actin and 36B4. The sequences for the primers are listed in Table I.

Measuring Protein Levels

Proteins were isolated in three steps: precipitation, washing, and solubilization. After phase separation, the organic phase was retained, and proteins were precipitated by the addition of absolute ethanol, followed by incubation at room temperature for 10 min. Samples were then centrifuged at 12,000× g for 10 min at 4°C to pellet the proteins.

The resulting protein pellet was washed three times with 0.3 M guanidine hydrochloride in 95% ethanol and once with 100% ethanol to remove residual phenol and other contaminants. Pellets were briefly air-dried and subsequently solubilized in phosphate-buffered saline (PBS) containing 1% SDS by

incubation at 50°C with intermittent vortexing until complete dissolution.

Total protein concentrations were quantified using a BCA protein assay kit (Thermo Fisher Scientific) according to the manufacturer's instructions. *UCP1*, *PPARγ*, and *PGC1-α* protein concentrations of protein extracts were measured using a Sandwich ELISA (13) kit *per* the manufacturer's instructions.

Table I

Primer sequences of target genes

Gene name	Primer sequences	
PPARγ	Forward	GTACTGTCGGTTTCAGAAGTGCC
	Reverse	ATCTCCGCCAACAGCTTCTCCT
C/EBPβ	Forward	GGTTTCGGGACTTGATGCA
	Reverse	CAACAACCCCGCAGGAAC
PGC1-α	Forward	GAATCAAGCCACTACAGACACCG
	Reverse	CATCCCTCTTGAGCCTTTCGTG
CIDEA	Forward	AGAAGGTCCTACTGACCCCC
	Reverse	ACCCGGTGTCCATTTCTGTC
FABP4	Forward	TGAAATCACCGCAGACGACAGG
	Reverse	GCTTGTCACCATCTCGTTTTCTC
UCP1	Forward	CCTGCCTCTCTCGGAAACAA
	Reverse	GTAGCGGGGTTTGATCCCAT
PRDM16	Forward	GATGGGAGATGCTGACGGAT
	Reverse	TGATCTGACACATGGCGAGG

Measuring triglyceride levels

The Triglyceride Colorimetric Assay kit was purchased from Cayman Chemical Company and was used for triglyceride quantification. The resulting absorbance was detected at 530 - 550 nm using a BioTek Synergy Htx plate reader. The concentration of triglycerides contained in each sample was calculated using the "triglyceride standard curve" created by using the absorbance values of standard solutions with known triglyceride concentrations.

Metabolomics

The cell culture samples were washed with PBS solution and centrifuged. The pellet was resuspended with homogenization buffer (10 mM Tris–HCl, 5 mM EDTA, 120 mM NaCl, at pH 7.4). Cells were disrupted with a homogenizer and centrifuged (14 min at 14,000× g and 4°C). Pellet (mainly containing nuclear and mitochondrial fractions) was discarded, and the supernatant was centrifuged for 1 h at 100,000× g and 4°C. Supernatant (cytosolic fraction) was stored at -80°C until analysis. Homogenised cell culture samples were diluted to contain 10,000 µg/mL protein for Metabolomics analysis. Three technical replicates were prepared for each sample. First, the diluted samples were extracted using a methanol-water mixture (8:1, v/v), and they were centrifuged. Then supernatant was evaporated to dryness, and the residues were methoxyamined and derivatized with MSTFA (N-Methyl-N-(trimethylsilyl) trifluoroacetamide) containing 1% TMCS (trimethylchlorosilane). After derivatization, the samples were transferred to GC-MS vials and analysed using a GC-MS instrument (Shimadzu GC-MS-QP2010 Ultra, JP) with a DB-5MS stationary phase column (30 m + 10 m DuraGuard × 0.25 mm i.d. and 0.25 µm film thickness). The mass range was from 50 to 650 Daltons. Data deconvolution, peak alignment, normalization (MSTUS), and data matrix generation were performed with MS-DIAL software (ver. 4.0). Metabolites were identified to a threshold of > 70% using a commercial library (Fiehn Retention Index Library). Metabolites with missing values of more than 50% of the samples were removed from the data matrix. Other missing values were filled with the half value of the lowest concentration in the metabolite group. The final version of the data matrix was uploaded to MetaboAnalyst software to perform multivariate statistical analyses. Multivariate analyses included partial least squares discriminant analysis (PLS-DA), variable importance in projection (VIP) analysis, and heat map analysis.

Statistical analyses

Statistical analysis was performed using SPSS version 22.0 (IBM Corp., USA). Before inferential analyses, data distribution was assessed for normality using the Shapiro–Wilk test, and homogeneity of variances was evaluated using Levene's test. For datasets meeting the assumptions of normality and homoscedasticity, one-way analysis of variance (ANOVA) was applied. When a significant main effect was observed, post-hoc comparisons were conducted using the least significant difference (LSD) test to compare predefined group differences. In cases where homogeneity of variances was violated, the Games–Howell post-hoc test was employed. For comparisons between two groups, Student's t-test was used for normally distributed data, whereas the Mann–Whitney U test was applied when normality assumptions were not met. Tukey's honestly significant difference (HSD) test was not applied, as the study primarily focused on planned comparisons

between treatment and control groups rather than all possible pairwise comparisons. All data were presented as numbers and percentages or as mean ± standard deviation (SD). A p-value < 0.05 was considered statistically significant.

Assay precision

For qPCR analysis, amplification efficiency was confirmed to be within 90 - 110%, and melt curve analysis verified primer specificity. The BCA protein assay and ELISA kits used to quantify *UCP1*, *PPARγ*, and *PGC1-α* had intra-assay coefficients of variation (CV) below 10%, ensuring high analytical reliability.

Sample size justification

Three biological replicates were used for each treatment group in accordance with standard practices for *in vitro* cell culture experiments. This sample size was considered adequate to detect significant biological differences in gene expression and metabolite levels under controlled laboratory conditions.

Results and Discussion

Gene expression levels and protein levels

PPARγ, *C/EBPβ*, and *FABP4*, which are key regulators of adipogenesis, exhibited similar gene expression levels ($p > 0.05$) during both the differentiation and maturation processes (Figure 1). However, when it comes to the key regulators of browning, including *PGC1α*, *CIDEA*, *UCP1*, and *PRDM16*, their gene expression levels varied among different groups (Figure 2). During the differentiation process, *UCP1* gene expression levels were higher in the 5 µM delphinidin group compared to other groups ($p < 0.05$). In the maturation process, *PRDM16* gene expression levels for delphinidin were higher in the 20 µM group ($p < 0.05$).

UCP1, *PGC1-α*, and *PPARγ* protein concentrations following delphinidin treatment during differentiation and maturation are presented in Table II. No significant differences were observed among delphinidin-treated groups or compared with control for *UCP1* protein levels in either the differentiation or maturation phases ($p > 0.05$). During the differentiation phase, *PGC1-α* protein levels in the 5 µM delphinidin group were significantly lower than those in the 20 µM group ($p < 0.05$), whereas no significant differences were observed between the 5 µM group and the 10 µM or control groups. During maturation, *PGC1-α* protein levels in the 5 µM group were significantly lower than in the 10 µM group ($p = 0.011$), while no significant difference was observed between the 5 µM group and the control. In the differentiation phase, *PPARγ* protein levels did not differ among delphinidin-treated groups; however, all delphinidin concentrations resulted in significantly lower *PPARγ* levels compared with the control group ($p < 0.05$). During maturation, *PPARγ* protein levels were significantly higher in all delphinidin-treated groups compared with the control ($p < 0.05$), with no significant differences observed between delphinidin doses.

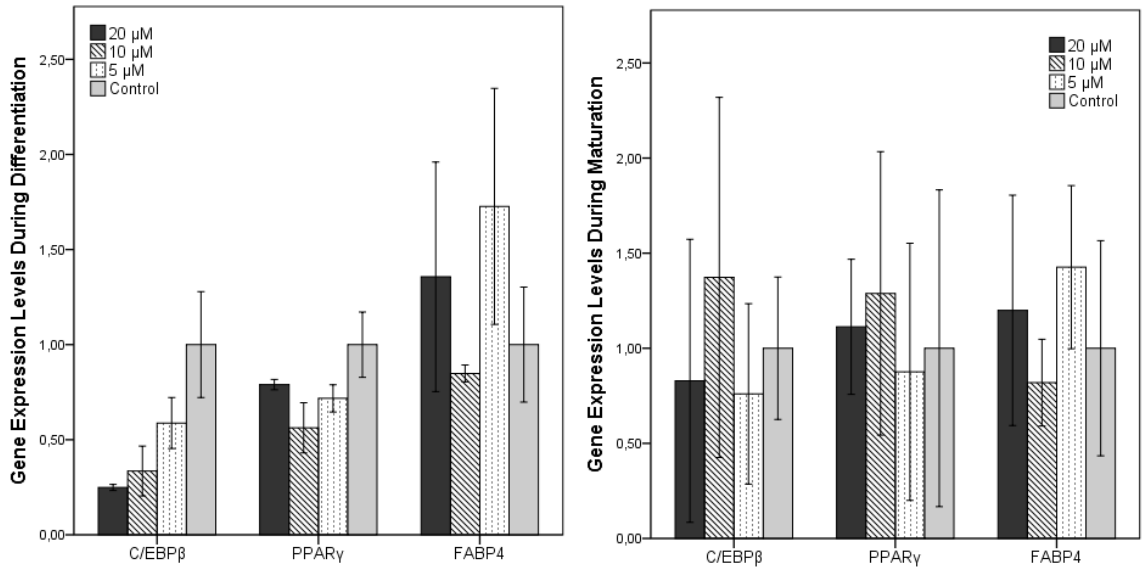

Figure 1.

C/EBPβ, *PPARγ*, and *FABP4* gene expression levels of delphinidin in the differentiation and maturation processes

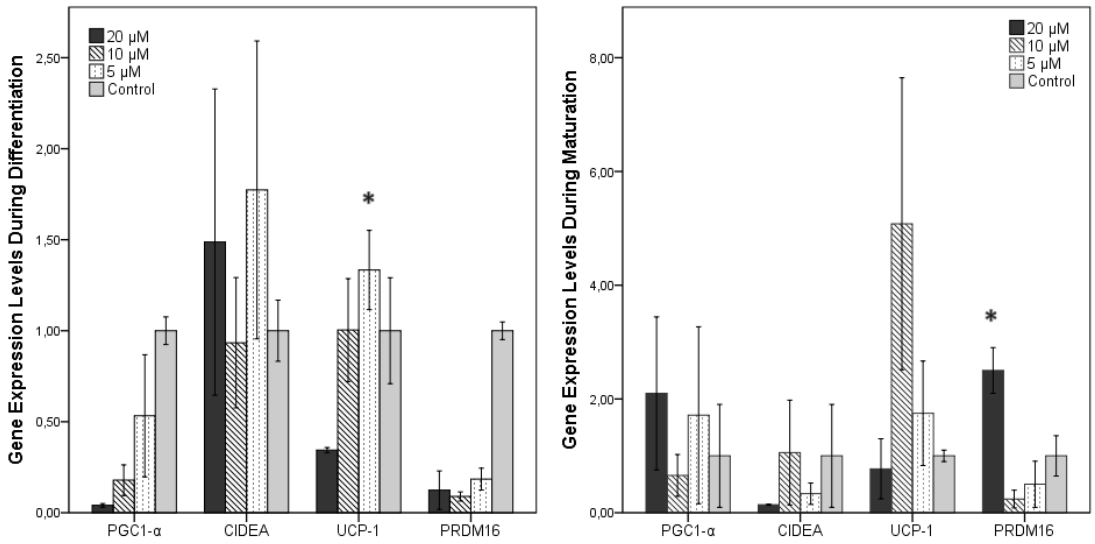

Figure 2.
PGC1-α, *CIDEA*, *UCP-1*, and *PRDM16* gene expression levels of delphinidin in the differentiation and maturation processes

Table II
Effects of delphinidin treatment on *UCP1*, *PGC1-α*, and *PPARγ* protein levels during adipocyte differentiation and maturation [1, 2, 3]

	Protein Levels (mg/dL)		
	UCP1	***PGC1-α***	***PPARγ***
Differentiation (Concentration, µM)			
20	46.1 ± 4.67 [a]	40.1 ± 4.20 [a]	75.7 ± 1.73 [a]
10	37.5 ± 3.42 [a]	36.8 ± 0.54 [a, b]	80.3 ± 2.52 [a]
5	37.5 ± 8.81 [a]	30.9 ± 0.65 [b]	80.0 ± 2.91 [a]
Control	40.6 ± 4.14 [a]	28.6 ± 0.86 [b]	88.6 ± 2.72 [b]
	p > 0.05	**p < 0.05**	**p < 0.05**
Maturation (Concentration, µM)			
20	33.5 ± 0.91 [a]	31.4 ± 1.82 [a, b]	86.3 ± 1.36 [a]
10	46.8 ± 17.64 [a]	34.0 ± 0.33 [a]	87.0 ± 1.53 [a]
5	41.0 ± 4.31 [a]	29.5 ± 0.33 [b]	85.2 ± 1.75 [a]
Control	35.1 ± 3.24 [a]	31.4 ± 0.75 [a, b]	72.9 ± 3.28 [b]
	p > 0.05	**p < 0.05**	**p < 0.05**

[1]Data were analyzed by one-way ANOVA, [2]Data are presented as mean ± SD,[3]Means within a column without a common letter differ, p < 0.05.

The differentiation of preadipocytes into adipocytes is tightly regulated by transcription factors, including *PPARγ* and *C/EBP*, required for growth arrest (14, 12). Two studies examined delphinidin's impact on *PPARγ*. In the first, 3T3-L1 cells treated with delphinidin (25 - 100 µM) reduced *PPARγ* mRNA and protein levels dose-dependently (10). In the second, delphinidin suppressed intermediate *PPARγ* markers (8). However, our study showed no significant change in *PPARγ* protein or mRNA levels, suggesting no anti-adipogenic effect, possibly due to lower dosage compared to other studies. *C/EBPβ*, a key transcription factor in early adipocyte differentiation (14), was examined in one study, which found that delphinidin significantly downregulated *C/EBPβ* and *C/EBPδ* expression in 3T3-L1 cells (8). *PPARγ* and *C/EBPα* expression are followed by the expression of adiponectin and fatty acid-binding protein 4 (*FABP4*), which are responsible for terminal differentiation and formation of the fat cell phenotype (14). While two studies suggest delphinidin as a potential anti-obesity agent due to its suppression of adipogenesis and mesenchymal stem cell adipogenesis (15), our data did not show a difference in *FABP4* expression. Further studies are needed to confirm its effect.

CIDEA regulates beige adipocytes, and it is associated with genes such as *PGC-1α* and *UCP1* involved in thermogenesis, during the transformation of *WAT* into *BAT* (16). Although no studies explore delphinidin's effect on *CIDEA* expression, anthocyanin oligomers significantly up-regulated *CIDEA* (15). *UCP1*, another key player in thermogenesis (17), lacks

delphinidin-specific research; however, anthocyanidins have shown potential in boosting energy expenditure by reducing mitochondrial respiration and dissipation of the mitochondrial proton gradient (18). In a recent study, after the treatment of beige-like adipocytes with anthocyanin-rich black soybean, the level of *UCP1* in mitochondria was fivefold higher than that in *WAT* (19). In contrast, the present study demonstrated that there was no significant difference in *UCP1* protein concentration. However, we observed the highest *UCP1* expression at 5 μM delphinidin-exposed cells during the differentiation stage. This result suggests delphinidin may have induced browning in 3T3-L1 adipocytes, especially in the early phase of adipogenesis, but not in a dose-dependent manner. However, the current study is the first to use only delphinidin, and it is limited to demonstrating the preventive role of delphinidin as a thermogenic compound in adipocytes.

PGC1-α, *PPARγ*, and *PRDM16* are known crucial regulators of browning and *UCP1* mRNA expression (17, 20). *PGC1-α* increased oxygen consumption *via* mitochondrial activation, and its expression increased in *BAT* (21). There are no studies on the effect of delphinidin on *PGC1-α*; however, there are limited studies evaluating the anthocyanidin effect on this protein. In a recent study, the expression of *PGC1-α* was dose-dependently increased by anthocyanin treatment (500 mg/kg/day) in cell culture of *BAT* from rats fed anthocyanins compared to that in *BAT* from non-fed rats (19). Similarly, 3T3-L1 cells increased *PGC-1α* protein levels after treatment with anthocyanin oligomers (15). In the present research, the protein concentration of *PGC1-α* was dose-dependently increased during maturation. However, delphinidin did not induce significant changes in *PGC-1α* gene expression at any stage. *PRDM16* is one of the key transcription factors that regulate the thermogenic gene program in brown and beige adipocytes (22). *PPARγ* deacetylation is strictly connected with the up-regulation of *PRDM16*, which promotes browning (23). To our knowledge, this is the first study to show the effect of delphinidin on *PRDM16*. There is only one study on the treatment of anthocyanin oligomers in 3T3-L1 that showed a significantly increased expression of the *PRDM16* gene and proteins (15). According to this study, this research showed an increased level of *PRDM16* during the maturation process, especially at high doses of delphinidin. Our results suggest that delphinidin has a browning effect on 3T3-L1 cells. It is necessary to conduct more studies to demonstrate the preventive role of delphinidin as a thermogenic compound in adipocytes.

Triglyceride levels

Triglyceride concentrations following delphinidin treatment during differentiation and maturation are shown in Table III. During differentiation, the 20 μM delphinidin group exhibited significantly higher triglyceride levels compared with the 10 μM, 5 μM, and control groups, and all groups differed significantly from each other ($p < 0.001$). During maturation, triglyceride levels in the 20 μM delphinidin group were significantly higher than those in the 10 μM and 5 μM groups ($p < 0.05$), while the 10 μM delphinidin group exhibited the lowest triglyceride concentration among all groups ($p < 0.05$). In *vitro* and in *vivo* studies have shown that treatment with delphinidin had a great inhibitory effect on intracellular triglyceride accumulation in a dose-dependent manner. The triglyceride accumulation in *HepG2* cells was reduced by 50% with 100 μM and 59% with 180 μM of delphinidin (24). Another study showed that 25, 50, and 100 μM of delphinidin reduced intracellular triglyceride accumulation in 3T3-L1 cells by 30%, 38%, and 58%, respectively (8). Black soybean seed coat extract reduced triglyceride levels significantly in mice with a high-fat diet and streptozotocin (STZ)-induced diabetes (25). However, some studies did not show an effect of delphinidin on triglyceride accumulation (26, 24, 27). In the present study, intracellular triglyceride accumulation was significantly reduced by delphinidin. However, triglycerides did not decrease in a dose-dependent manner. Interestingly, in both processes, 10 μM of delphinidin reduced intracellular triglyceride accumulation more than 20 μM. Moreover, 10 μM reduced triglyceride levels in the maturation process (67%) instead of the early differentiation process (46%). A possible reason for this result could be the delayed effect of delphinidin treatment on cell cycle progression. The lipid-lowering effect of delphinidin is largely attributed to the early stage of adipogenesis, but in the present study, the positive effect of delphinidin appears in the intermediate and late adipogenesis phases.

Table III

Effects of delphinidin treatment on intracellular triglyceride levels during adipocyte differentiation and maturation [1, 2, 3]

	Triglyceride Concentration (mg/dL)	
	Differentiation	**Maturation**
Delphinidin Concentration (μM)		
20	67.7 ± 1.10 [a]	29.4 ± 2.21 [a]
10	28.8 ± 1.33 [b]	17.7 ± 1.55 [c]
5	43.2 ± 3.54 [c]	21.5 ± 1.99 [c]
Control	52.9 ± 0.88 [d]	52.9 ± 0.88 [b]
	p < 0.001	**p < 0.05**

[1]Data were analyzed by one-way ANOVA. [2]Data are presented as mean ± SD. [3]Means within a column without a common letter differ, $p < 0.05$.

Metabolomics

The GC-MS-based Metabolomics analysis identified 205 metabolites in cell samples. Only 37 of these

metabolites were identified, and the changes between the groups were statistically analyzed. During the differentiation process, fifteen of these metabolites exhibited significant alterations between the control groups ($p < 0.05$). To examine the differences in metabolomic profiles between the various groups in detail, a PLS-DA score plot was created to illustrate the distinctions in metabolite profiles between the control group (DFDK) and the lowest concentration of delphinidin treatment (5 µM) in our study (DFD5) (Figure 3a). A VIP graph was also utilized in order to identify the metabolites affecting differentiation in the PLS-DA score plot (Figure 3b). From GC-MS-based metabolomics profile analysis results, levels of glyceraldehyde, alanine, porphine, linoleic acid, and glycine were found to be different in terms of importance. During the maturation process, two of the identified metabolites were significantly altered between the control groups ($p < 0.05$). The PLS-DA score plot presented partially similar metabolomic profiles between groups (Figure 4a). A VIP graph was also utilized in order to identify the metabolites affecting differentiation in the PLS-DA score plot (Figure 4b). From GC-MS-based metabolomics profile analysis results, levels of mannose, p-cresol, threitol, talose, and glycerol were found to be different in order of importance.

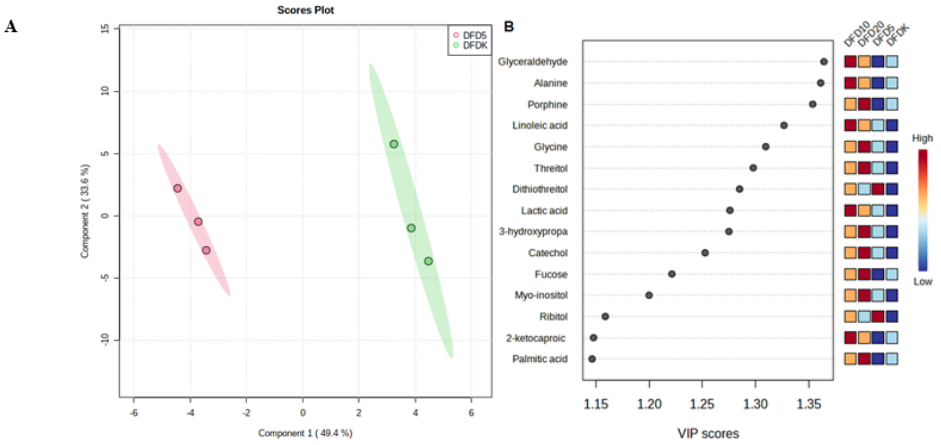

Figure 3.

Metabolic profiles obtained by GC-MS for delphinidin and control groups in the differentiation process: (A) Partial least squares differential analysis (PLS-DA) score graph; (B) Variable importance in projection (VIP) charts of metabolites that are effective in separating the 20, 10, 5 µM delphinidin and control groups.

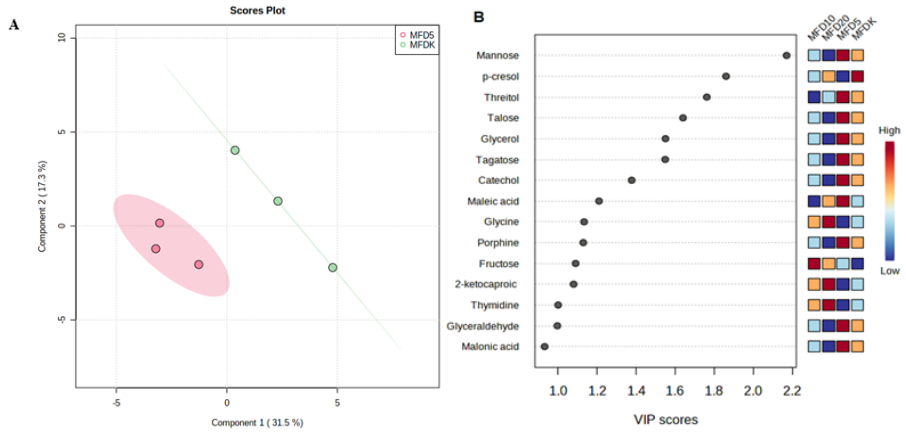

Figure 4.

Metabolic profiles obtained by GC-MS for delphinidin and control groups in the maturation process: (A) Partial least squares differential analysis (PLS-DA) score graph; (B) Variable importance in projection (VIP) charts of metabolites that are effective in separating the 20, 10, 5 µM delphinidin and control groups.

This study is the first to show the effect of delphinidin treatment on metabolic pathways in 3T3-L1 cells. During the differentiation process, the metabolite significantly increased with delphinidin was glyceraldehyde, a triose monosaccharide intermediate in the metabolism of fructose (28). Glyceraldehyde is highly reactive and can modify and cross-link proteins, which are cytotoxic and inhibit intracellular glutathione levels (29). The

study suggests that delphinidin might affect fructose metabolism only in lower concentrations.

During maturation, the mannose metabolite significantly changed. It belongs to the class of organic compounds known as hexose phosphates (30). Mannose is involved in a number of enzymatic reactions; in particular, it can be converted into fructose 6-phosphate through its interaction with the enzyme mannose-6-phosphate isomerase. Mannose inhibits adipogenic differentiation and regulates glucose metabolism (31). Our results suggest that 5 µM delphinidin-treated cells could be more effective. Surprisingly, the higher levels of delphinidin show lower levels of mannose. Therefore, delphinidin could positively reduce adipogenic differentiation at a lower dose. To further explore the role of delphinidin with metabolites, more studies are necessary, where metabolomic analyses were carried out using both GC-MS and liquid chromatography-quadrupole time-of-flight mass spectrometry (LC-qTOF-MS) methods.

Conclusions

Plant-based bioactive compounds show potential in anti-obesity effects, however, research on delphinidin is limited. Our study explored delphinidin's effects on 3T3-L1 preadipocytes, indicating its potential to contribute to browning by increasing *UCP1* and *PRDM16* expression and reducing triglyceride levels during maturation. However, we did not observe any effects of delphinidin on the key expressions of beige-specific genes (*PPARγ*, *PGC1-α,* and *CIDEA*). Additionally, the impact on metabolites such as glyceraldehyde, alanine, porphine, mannose, and p-cresol remains uncertain. While our foodomics approach offers valuable insights into the potential of delphinidin as a dietary supplement for obesity management, further in-depth in *vitro* and in *vivo* studies are essential to fully elucidate its browning effects and therapeutic viability.

Acknowledgement

The authors thank TUBITAK for supporting this project (project number 220S742).

Funding

This work was supported by TUBITAK 1001-The Scientific and Technological Research Projects Funding Program [project no. 220S742].

Availability of data and materials

The data supporting the present study will be made available on request from the corresponding author.

Ethics approval and consent to participate

Not applicable.

AI use disclosure

Not applicable.

Conflict of interest

The authors declare no conflict of interest.

Abbreviations

Uncoupling Protein 1 (*UCP1*); Peroxisome Proliferator-Activated Receptor Gamma (*PPARγ*); CCAAT/Enhancer Binding Protein Beta (*C/EBPβ*); Peroxisome Proliferator-Activated Receptor Gamma Coactivator 1-Alpha (*PGC1-α*); Cell Death-Inducing DNA Fragmentation Factor-Like Effector A (*CIDEA*); Fatty Acid Binding Protein 4 (*FABP4*); PR Domain Containing 16 (*PRDM16*); 3-Isobutyl-1-methylxanthine (IBMX); Dimethyl Sulfoxide (DMSO); Dulbecco's Modified Eagle's Medium (DMEM); Fetal Bovine Serum (FBS); Brown Adipose Tissue (BAT); White Adipose Tissue (WAT); Gas Chromatography–Mass Spectrometry (GC-MS); Partial Least Squares Discriminant Analysis (PLS-DA); Variable Importance in Projection (VIP); Quantitative Polymerase Chain Reaction (qPCR); Phosphate-Buffered Saline (PBS).

References

1. Valdés A, Álvarez-Rivera G, Socas-Rodríguez B, Herrero M, Ibáñez E, Cifuentes A. Foodomics: Analytical Opportunities and Challenges. Analytical Chemistry. 2022;94(1):366-381.
2. Ortea I. Foodomics in health: Advanced techniques for studying the bioactive role of foods. TrAC Trends in Analytical Chemistry. 2022;150:116589.
3. Chen Z, Zhang R, Shi W, Li L, Liu H, Liu Z, et al. The Multifunctional Benefits of Naturally Occurring Delphinidin and Its Glycosides. J Agric Food Chem. 2019;67(41):11288-11306.
4. Khoo HE, Azlan A, Tang ST, Lim SM. Anthocyanidins and anthocyanins: colored pigments as food, pharmaceutical ingredients, and the potential health benefits. Food Nutr Res. 2017;61(1):1361779.
5. Cremonini E, Daveri E, Mastaloudis A, Adamo AM, Mills D, Kalanetra K, et al. Anthocyanins protect the gastrointestinal tract from high fat diet-induced alterations in redox signaling, barrier integrity and dysbiosis. Redox biology. 2019;26:101269.
6. Daveri E, Cremonini E, Mastaloudis A, Hester SN, Wood SM, Waterhouse AL, et al. Cyanidin and delphinidin modulate inflammation and altered redox signaling improving insulin resistance in high fat-fed mice. Redox biology. 2018;18:16-24.
7. Sandoval V, Femenias A, Martínez-Garza Ú, Sanz-Lamora H, Castagnini JM, Quifer-Rada P, et al. Lyophilized Maqui (*Aristotelia chilensis*) Berry

Induces Browning in the Subcutaneous White Adipose Tissue and Ameliorates the Insulin Resistance in High Fat Diet-Induced Obese Mice. Antioxidants (Basel). 2019;8(9):360.
8. Rahman N, Jeon M, Kim YS. Delphinidin, a major anthocyanin, inhibits 3T3-L1 pre-adipocyte differentiation through activation of Wnt/β-catenin signaling. BioFactors (Oxford, England). 2016;42(1):49-59.
9. Kim HK, Kim JN, Han SN, Nam JH, Na HN, Ha TJ. Black soybean anthocyanins inhibit adipocyte differentiation in 3T3-L1 cells. Nutrition research (New York, NY). 2012;32(10):770-777.
10. Yunas RW, Rahmawati SI, Saputri FC, Indriani DW, Bayu A, Putra MY. Antihypertensive effects of Hibiscus sabdariffa and Zingiber officinale var. Rubrum extracts in a deoxycorticosterone acetate-salt induced hypertension rat model. Farmacia. 2024;72(6):1299-1307.
11. Park M, Sharma A, Lee HJ. Anti-Adipogenic Effects of Delphinidin-3-O-β-Glucoside in 3T3-L1 Preadipocytes and Primary White Adipocytes. Molecules (Basel, Switzerland). 2019;24(10): 1848.
12. Wu T, Tang Q, Gao Z, Yu Z, Song H, Zheng X, et al. Blueberry and mulberry juice prevent obesity development in C57BL/6 mice. PLoS One. 2013;8(10):e77585.
13. Aglago EK, Huybrechts I, Murphy N, Casagrande C, Nicolas G, Pischon T, et al. Consumption of Fish and Long-chain n-3 Polyunsaturated Fatty Acids Is Associated With Reduced Risk of Colorectal Cancer in a Large European Cohort. Clinical Gastroenterology and Hepatology. 2020;18(3):654-666.
14. Farmer SR. Transcriptional control of adipocyte formation. Cell metabolism. 2006;4(4):263-273.
15. Choi M, Mukherjee S, Yun JW. Anthocyanin oligomers stimulate browning in 3T3-L1 white adipocytes via activation of the β3-adrenergic receptor and ERK signaling pathway. Phytotherapy research : PTR. 2021;35(11):6281-6294.
16. Jash S, Banerjee S, Lee M-J, Farmer SR, Puri V. CIDEA Transcriptionally Regulates UCP1 for Britening and Thermogenesis in Human Fat Cells. iScience. 2019;20:73-89.
17. Bonet ML, Oliver P, Palou A. Pharmacological and nutritional agents promoting browning of white adipose tissue. Biochimica et biophysica acta. 2013;1831(5):969-985.
18. Skates E, Overall J, DeZego K, Wilson M, Esposito D, Lila MA, et al. Berries containing anthocyanins with enhanced methylation profiles are more effective at ameliorating high fat diet-induced metabolic damage. Food and chemical toxicology: an international journal published for the British Industrial Biological Research Association. 2018;111:445-453.
19. Lee M, Lee M. The Effects of C3G and D3G Anthocyanin-Rich Black Soybean on Energy Metabolism in Beige-like Adipocytes. Journal of agricultural and food chemistry. 2020;68(43):12011-12018.
20. Richard D, Picard F. Brown fat biology and thermogenesis. Frontiers in bioscience (Landmark edition). 2011;16(4):1233-1260.
21. Gill JA, La Merrill MA. An emerging role for epigenetic regulation of Pgc-1α expression in environmentally stimulated brown adipose thermogenesis. Environmental epigenetics. 2017;3(2):dvx009.
22. Saulite L, Jekabsons K, Klavins M, Muceniece R, Riekstina U. Effects of malvidin, cyanidin and delphinidin on human adipose mesenchymal stem cell differentiation into adipocytes, chondrocytes and osteocytes. Phytomedicine : international journal of phytotherapy and phytopharmacology. 2019;53:86-95.
23. Bargut TCL, Souza-Mello V, Aguila MB, Mandarim-de-Lacerda CA. Browning of white adipose tissue: lessons from experimental models. Horm Mol Biol Clin Investig. 2017 Jan 18;31(1):20160051.
24. Parra-Vargas M, Sandoval-Rodriguez A, Rodriguez-Echevarria R, Dominguez-Rosales JA, Santos-Garcia A, Armendariz-Borunda J. Delphinidin Ameliorates Hepatic Triglyceride Accumulation in Human HepG2 Cells, but Not in Diet-Induced Obese Mice. Nutrients. 2018;10(8): 1060.
25. Chen Z, Wang C, Pan Y, Gao X, Chen H. Hypoglycemic and hypolipidemic effects of anthocyanins extract from black soybean seed coat in high fat diet and streptozotocin-induced diabetic mice. Food & function. 2018;9(1):426-439.
26. Aboufarrag H, Hollands WJ, Percival J, Philo M, Savva GM, Kroon PA. No Effect of Isolated Anthocyanins from Bilberry Fruit and Black Rice on LDL Cholesterol or other Biomarkers of Cardiovascular Disease in Adults with Elevated Cholesterol: A Randomized, Placebo-Controlled, Cross-Over Trial. Molecular nutrition & food research. 2022;66(21):e2101157.
27. van der Heijden RA, Morrison MC, Sheedfar F, Mulder P, Schreurs M, Hommelberg PPH, et al. Effects of Anthocyanin and Flavanol Compounds on Lipid Metabolism and Adipose Tissue Associated Systemic Inflammation in Diet-Induced Obesity. Mediators of Inflammation. 2016;2016:2042107.
28. Mayes PA. Intermediary metabolism of fructose. The American journal of clinical nutrition. 1993;58(5 Suppl):754s-765s.
29. Usui T, Shizuuchi S, Watanabe H, Hayase F. Cytotoxicity and oxidative stress induced by the glyceraldehyde-related Maillard reaction products for HL-60 cells. Bioscience, biotechnology, and biochemistry. 2004;68(2):333-340.
30. Wood FC, Jr., Leboeuf B, Renold AE, Cahill GF, Jr. Metabolism of mannose and glucose by adipose tissue and liver slices from normal and alloxan-diabetic rats. The Journal of biological chemistry. 1961;236:18-21.
31. Sharma V, Ichikawa M, Freeze HH. Mannose metabolism: more than meets the eye. Biochemical and biophysical research communications. 2014;453(2):220-228.